Path Planning and Cooperative Control for Automated Vehicle Platoon Using Hybrid Automata

Zichao Huang, Duanfeng Chu, Chaozhong Wu, and Yi He

***Abstract*— Cooperative driving systems may increase the utilization of road infrastructure resources through coordinated control and platooning of individual vehicles with the potential of enhancing both traffic safety and efficiency. Vehicle cooperative driving is essentially a hybrid system that is a combination of discrete events, i.e., the transition of discrete cooperative maneuvering modes, such as vehicle merging and platoon splitting, as well as continuous vehicle dynamics. In this paper, a novel hybrid system consisting of the discrete cooperative maneuver switch and the continuous vehicle motion control is introduced into a multi-vehicle cooperative control system with a distributed control structure, leading each automated vehicle to conduct path planning and motion control separately. The primary novelty of this paper lies in that it presents a control algorithm combining artificial potential field (APF) approach with model predictive control (MPC), and using the optimizer of the MPC controller to replace the gradient-descending method in the traditional APF approach. Such a method can accomplish both path planning and motion control synchronously. Second, based on hybrid automata, a cooperative maneuver switching model consisting of a system state set and a discrete maneuver transition rule is established for two discrete maneuvers in the cooperative driving system, i.e., single-vehicle cruising and multiple-vehicle platooning. Simulations in several typical traffic scenarios demonstrate the effectiveness of the proposed method.**

***Index Terms*— Automated vehicle platoon, path planning and tracking, model predictive control, artificial potential field.**

I. Introduction

OVER the past few decades, the increasing vehicle volume has caused serious issues on traffic safety, congestion and environmental pollution. Studies show that more than 90% of vehicle crashes are caused by human errors [1]. Automated driving technology is currently recognized as one of the possible solutions that may have great potential to improve road traffic safety and efficiency [2], [3]. Automated vehicles usually utilize onboard sensors such as LiDAR, Radar and/or camera to sense traffic environmental information for path planning, and then to conduct vehicle motion control to track the planned path. Currently, there are numerous studies that have made significant progress on some key technologies of a single vehicle's automatic control, such as Adaptive Cruise Control (ACC) [4], Automated Emergency Braking (AEB) [5]–[7], Lane Keeping Assist (LKA) [8], [9], etc. Generally, the performances of such automatic controllers depend largely on the measurement accuracies and ranges of onboard sensors. Some studies indicated that the fully autonomous vehicles would have to be driven millions of miles to demonstrate their reliability [10]. So how to improve the practicality of such sensor-based automated vehicles has become an important issue. Since the rapid development of wireless communication technologies, like Dedicated Short-Range Communication (DSRC) and the cellular communication LTE-V/5G, cooperative driving technology has gradually attracted many researchers' attentions.

Some benefits of communication-enabled cooperative driving system (CDS) can be identified relative to the single vehicle automated driving. Firstly, wireless radio waves can travel long distances and through obstacles which can greatly expand the detection range to provide unprecedented field of view of the driving environment. For example, Kim *et al.* [11] proposed a multi-vehicle cooperative driving system architecture using cooperative perception that can extend the sensing range to the union of all connected vehicles. Secondly, through reliable V2X (vehicle-to-everything), i.e. vehicle-to-vehicle (V2V) and vehicle-to-infrastructure (V2I) communications, information that can be shared among vehicles and infrastructures can be richer and with higher quality than the measured or estimated remotely using onboard sensors [12], [13]. Besides vehicle motion states, each vehicle's expected maneuvers can be shared with others directly, rather than its estimations of surrounding vehicles' information. At last, communication allows vehicles to coordinate their maneuvers for safety or efficiency goals such as collision avoidance and platooning. There are also some problems with using network communication in a CDS such as transmission

Manuscript received September 6, 2017; revised February 27, 2018; accepted May 6, 2018. Date of publication July 13, 2018; date of current version February 28, 2019. This work was supported in part by the National Natural Science Foundation of China under Grant 51675390, Grant U1764262, Grant 51605350, and Grant 51775396, in part by the Natural Science Foundation of Hubei Province under Grant 2017CFA0080, in part by the Fundamental Research Funds for the Central Universities under Grant 2017II50GX and Grant 2017IVB075, and the State Key Laboratory of Automotive Safety and Energy under Grant KF1807. The Associate Editor for this paper was P. Kachroo. *(Corresponding author: Duanfeng Chu.)*

Z. Huang is with the Research Institute of Highway, Ministry of Transport, Beijing 100088, China, and also with the Intelligent Transportation Systems Research Center, Wuhan University of Technology, Wuhan 430063, China.

D. Chu is with the Intelligent Transportation Systems Research Center, Wuhan University of Technology, Wuhan 430063, China, and also with the State Key Laboratory of Automotive Safety and Energy, Tsinghua University, Beijing 100084, China (e-mail: chudf@whut.edu.cn).

C. Wu and Y. He are with the Intelligent Transportation Systems Research Center, Wuhan University of Technology, Wuhan 430063, China, and also with the Engineering Research Center for Transportation Safety, Ministry of Education, Wuhan 430063, China.

Digital Object Identifier 10.1109/TITS.2018.2841967

delays, limited bandwidth of the network, and the same medium sharing problem. Related research has already been conducted on solving these problems. Öncü *et al.* [14] designed a Networked Control System framework for analyzing the effects of wireless communication between vehicles on CACC string stability performance. Harfouch *et al.* [15] present an Adaptive Switched Control Approach to deal with the heterogeneous platooning with Inter-Vehicle Communication Losses. The cooperative driving technology, however, can be an effective way to enhance the performance of automated vehicles in combination with path planning and tracking control with V2X information in the long run [16], [17].

Many CDSs attempt to form multiple vehicles into a platoon. A CDS platoon is a group of vehicles consisting of a leader which guides the platoon on the road, and followers which follow their preceding vehicles at short distances. The platooning of automated vehicles has the ability of increasing traffic throughput and reducing fuel consumption due to higher average cruising speeds, shorter inter-vehicle gaps, and lower air drags [3]. Generally, in order to develop a CDS, two main problems need addressing: the first one is the coordination of every single vehicle controller's actions; and the second one is the distributed control of each automated vehicle [18].

For the first problem, i.e. inter-vehicle cooperation, it is essential to establish a suitable system architecture. Most researchers believe that CDS is a hybrid system which includes both discrete cooperative maneuver switches and continuous motion control. Cassandras indicated that a hybrid system architecture is often natural to hierarchically decompose systems into lower-level components representing physical processes characterized by time-driven dynamics and a higher-level component representing discrete events related to these physical processes [19]. Researchers from the PATH group at University of California at Berkeley conducted a series of studies on automated highway system, which is an early version of CDS [20]–[22]. They proposed a five-layer distributed control architecture, including network, link, coordination, regulation, and physical layers, and the idea of the hierarchical control architecture was widely used in the subsequent studies of other cooperative driving systems [18], [23]. Same as the PATH group, Iftekhar *et al.* regarded the automated driving platoon as multi-objective flocking and proposed a multi-agent model to perform split/rejoin maneuvers. Meanwhile, they indicated that the whole framework was a hybrid system with a finite number of discrete states related to the corresponding driving modes [24]. In general, the task of a CDS is to guarantee the vehicle controller to execute the right maneuvers at the right time, such as cruising, merging, splitting, lane changing, overtaking, and so on.

The second problem is the distributed execution of specific maneuvers for a vehicle according to the cooperative algorithm. It can be solved by accomplishing the procedure of path planning and tracking. For road vehicles, the primary task of path planning is to ensure safety. Research in the area of path planning can be generally divided into two classes of methodologies which are global and local. Global methodologies have several disadvantages especially the intensive computation. It generally suites only for off-line path planning and cannot be used for real-time obstacle avoidance. The main advantage of local techniques is that they are much less computationally demanding than global ones. Thus they can be used in real-time control. For local methods, there are generally two technical types. One is based on the method of geographic information and the other is based on the artificial potential field (APF). Although the APF originated in the robot obstacle avoidance field [25], many researchers now apply the APF method to the path planning of autonomous vehicles due to its simplicity and elegance [26]–[28]. Wolf *et al.* proposed an APF function consisting of lanes, roads, vehicles, and speed functions for path planning and obstacle avoidance on autonomous or semi-autonomous vehicles on motorways. However, they did not consider the vehicle model when planning the path [29]. Trajectory tracking refers to the vehicle longitudinal and lateral coupling controller to generate the corresponding control actions and driving the vehicle to complete the planned path tracking. Li *et al.* [30] proposed an integrated local trajectory planning and tracking control framework to let the vehicle smoothly follow the reference path. String stability is an important property of platooning. Unlike most other studies, Guo *et al.* [31] designed an adaptive distributed controller for a heterogeneous vehicle platoon and analyzed the string stability. There are a lot of researches on the cooperative maneuver control algorithm [32]–[38]. However, current studies on CDS often decompose the task of the cooperative driving into a variety of automated vehicle control maneuvers mentioned above. These studies tend to regard these maneuvers as relatively independent ones. To achieve a better agility for automated vehicles, these maneuvers should not be controlled separately. For instance, the adaptive cruise maneuver not only needs to execute lane keeping, but also needs to overtake when an obstacle vehicle suddenly appears in front of the host vehicle. Therefore, it is important to present a unified algorithm that can make automated vehicles capable of dealing with general traffic scenarios.

Assuming that automated vehicles have already been equipped with onboard sensors and wireless communication modules to obtain rich information of their surrounding environments and motion states of their own. This paper proposes a distributed hybrid control architecture based on the hybrid dynamic characteristics of the multi-vehicle cooperative driving system using hybrid automata. A multi-vehicle cooperative control system is introduced based on the combination of APF and MPC. The contributions of this paper are as follows. First of all, based on the information from onboard sensors and wireless communications, an APF model is established and it is capable of describing the mutual effect and collaboration between a vehicle and its surrounding environment effectively. Afterwards, a MPC controller incorporating APF is presented to accomplish the path planning and motion control synchronously. Such a controller is designed from an optimization that takes vehicle kinematic constraints and safety into consideration. At last, it built a hybrid automaton model with a discrete maneuver transition rule consisting of a two-maneuver switch, i.e., single-vehicle cruising and

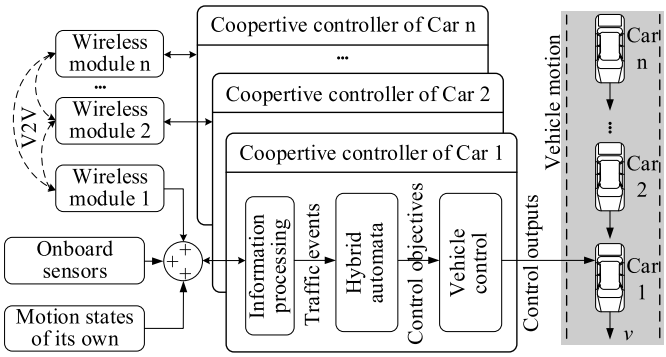

Fig. 1. Sketch of the cooperative control system.

multiple-vehicle platooning, to achieve the cooperative driving of automated vehicle platooning.

The reminder of this paper is organized as follows. In Section II, we sketch the system architecture of the automated vehicle platooning. In Section III, the model of artificial potential field for the cooperative driving system is presented. The MPC controller combining APF is designed in Section IV and a hybrid automaton model is built in Section IV. In Section V, a case study is used to validate the proposed algorithm. Section VI shows the simulation result analysis and the paper is concluded in the last section.

II. System Architecture of Automated Vehicle Platooning

In a cooperative driving system, automated vehicles can not only drive autonomously and safely using onboard sensors, but also have the function of platooning with neighboring automated vehicles through cooperation using V2V. As shown in Fig. 1, cooperative controllers for automated vehicles in a platoon consist of three functional parts: 1) processing the combined information including vehicle motion states and traffic environment through onboard sensors and V2V; 2) generating control objectives and constraints for a vehicle maneuver transition rule based on hybrid automata model under the current traffic events; 3) outputting control commands, i.e. steering angle and longitudinal acceleration to accomplish a vehicle's lateral and longitudinal motion control.

The cooperative control for automated vehicle platoons has two tasks: continuous vehicle motion control and discrete maneuver transition rule. In this study, a hybrid system which consists of the continuous vehicle system states and the discrete maneuver transitions is modeled based on hybrid automata.

For simplifying the discrete maneuver transitions of automated vehicles and the system control structure, here we focus on a two-maneuver switching logic with single-vehicle cruising and multiple vehicle platooning. That's to say, each vehicle either travels in a platoon, or cruises alone. As is shown in Fig. 2, the hybrid system is modeled with the transition of two discrete maneuvers including the platoon-splitting maneuver for single-vehicle cruising and the merging maneuver for multiple-vehicle platooning, as well as the continuous vehicle motion control based on MPC method. Therefore, the only functional difference between these two MPC controllers is the headway keeping, with the same terms in the MPC control's cost function, i.e., the vehicle model, the artificial potential field (APF) model and the constraint conditions. Moreover, the APF model is in charge of the traffic environment perception to generate an optimal trajectory for the path planning of an automated vehicle.

III. Vehicle Path Planning Based on the Artificial Potential Field Approach

The artificial potential field approach has been firstly presented by Khatib in the research of robots' collision avoidance which is a path-planning problem [25]. The artificial potential field generally consists of a "bowl-like" attractive field which forces objects to reach and a "mountain-like" repulsive field towards which forces objects to the contrary direction. Due to its human-like perception characteristic, this approach has become a popular method for path-planning of robots.

An automated vehicle alike a mobile robot can avoid obstacles by tracking the generated trajectory using the APF approach. In this case, a well-designed shape of the repulsive field representing obstacles ahead plays a crucial role for the obstacle avoidance effectiveness. The repulsive field always has an influence region where the shorter the distance to the target obstacle, the greater the repulsive force is. Moreover, outside the influence region, the repulsive force will rapidly reduce to the minimum or zero. Mathematically, the shape of the repulsive field is defined as a function with two independent variables, i.e. the limit distance of the potential field influence and the shortest distance to the target obstacle.

A. Structure of the Artificial Potential Field Model for Road Environments

Generally, automated vehicles' safety and mobility can be affected by two kinds of objects, i.e. neighboring vehicles and traffic line marks. The information of these target objects is obtained via on-board sensors and V2V communication. Therefore, we have designed an artificial potential field function to calculate the potentialsu_{mn} at a point (m, n) in the road environments, which includes three parts as follows [29].

$$u_{mn} = e_{mn} + r_{mn} + s_{mn} \tag{1}$$

where, e_{mn}, r_{mn} ands_{mn} represent a subject vehicle's potentials induced by an obstacle vehicle, neighboring traffic line marks, and the driving direction which exerts potential on the vehicle to drag it forward, respectively.

B. Potential of an Obstacle Vehicle

By modeling the influence of a neighboring obstacle vehicle, it is effective to keep a safe distance between the subject and an obstacle vehicle. Due to road geometric and vehicle dynamic features, hazardous levels of an obstacle vehicle's surrounding sections are distributed unevenly. For instance, the lateral hazardous levels of an obstacle vehicle mainly lie on the relative distance between two vehicles, but the longitudinal hazardous levels lie on the relative speed besides the relative

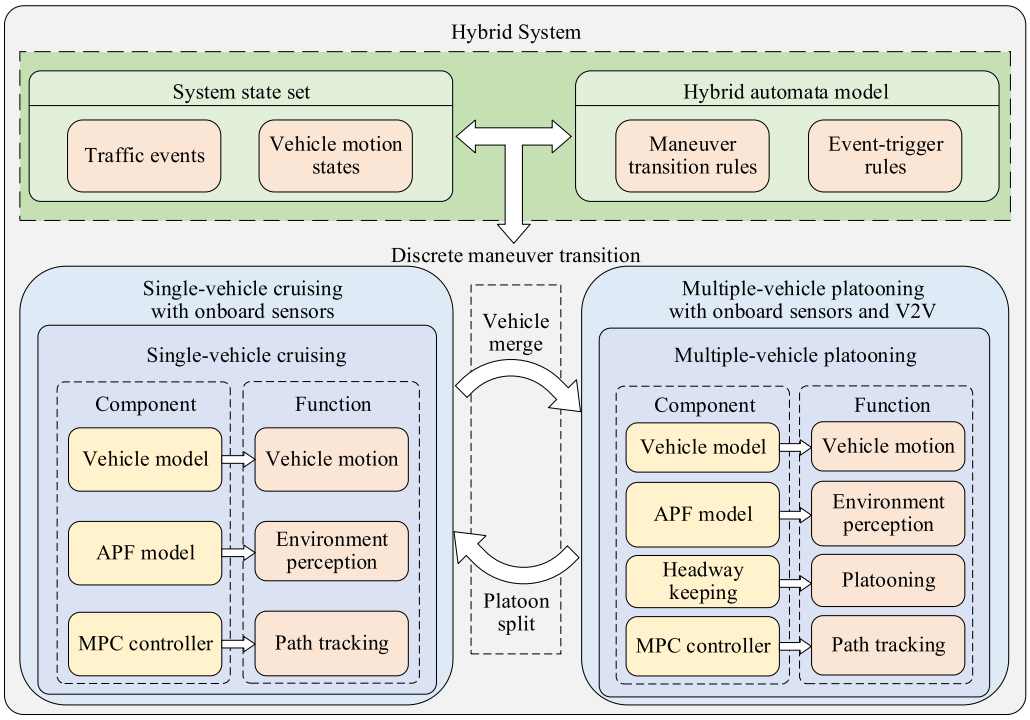

Fig. 2. Cooperative control for automated vehicle platoons based on hybrid automata.

distance. Therefore, we use different functions to describe the artificial potential field model of an obstacle vehicle in its longitudinal and lateral directions. Specifically, the influence of an obstacle vehicle is described to extend laterally, but using its longitudinal influence as a mainframe.

The modeling of the potential of an obstacle vehicle is carried out based on the coordinate system with the origin at the midpoint of the end of the vehicle's body frame and the x direction at its longitudinal movement, which is shown in Fig. 3. We use the bold solid line to describe the mainframe of an obstacle vehicle's longitudinal influence represented as a piecewise function as follows.

$$A_{car} = \begin{cases} U_{car}, & p \in \beta \\ v_r/(K-S), & (p \in \alpha) \cap (v_r > 0) \\ 0, & (p \in \alpha) \cap (v_r \le 0). \end{cases} \tag{2}$$

where, U_{car} is a constant of the maximum value of a vehicle's potential. v_r and K represent the relative speed and the relative distance, respectively, between the subject vehicle and its obstacle vehicle. When they move in the same direction, $v_r > 0$ if the subject vehicle moves faster than its obstacle vehicle, then $v_r < 0$ conversely. S is a safe clearance which is preset as $v_r \cdot \Delta T + S_{min}$, where ΔT is the time delay due to sensors and calculations and S_{min} is a given minimal safe clearance.

As shown in the lower part of Fig. 3 and Eq. (2), the potential value A_{car} of a point p like p_2 located at the section β in an obstacle vehicle's longitudinal direction is a constant U_{car}. For a point like p_1 belongs to the section α, A_{car} is equal to 0 when the relative speed $v_r \le 0$, and equal to $v_r/(K-S)$ otherwise. It reveals that the potential's value is negatively

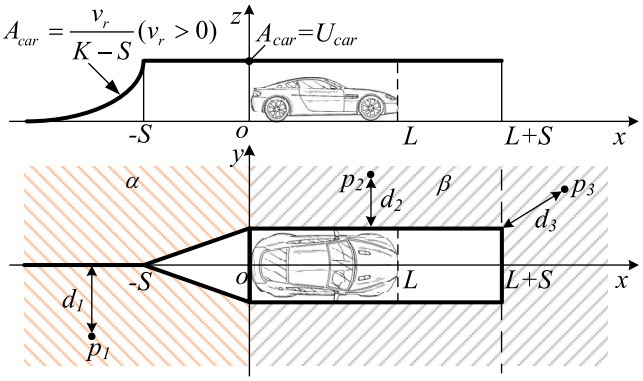

Fig. 3. Sketch of the artificial potential field modeling of an obstacle vehicle.

correlated to the relative distance, but positively correlated to the relative speed of the subject vehicle and its obstacle vehicle.

The potential of an obstacle vehicle in the lateral direction of the subject vehicle is extended towards two sides of the obstacle vehicle by using its longitudinal influence as the mentioned mainframe. We use a Gauss-type function which is exponentially correlated to the equivalent relative distance. Combining Eq. (2) and the potential calculation algorithm, we can obtain the total potential in both directions as follows.

$$e_{mn} = A_{car} \cdot \exp\left(-D^2/2\sigma_v^2\right). \tag{3}$$

where, see the lower part of Fig. 3, the equivalent relative distance D is the Euclidean distance between the frontal influence point p_3 and the obstacle vehicle contour's edge, or the relative distance in the lateral direction of the obstacle vehicle

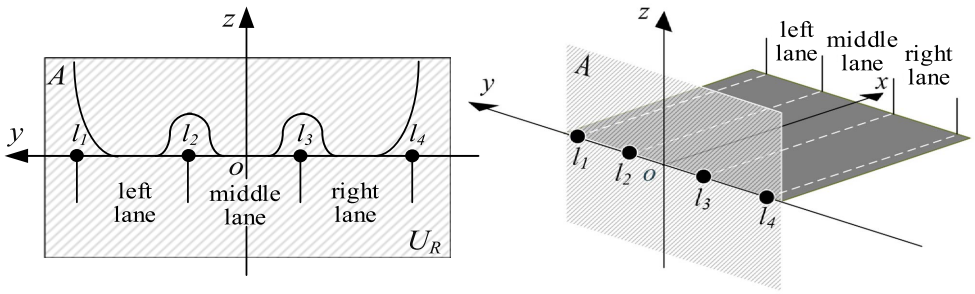

Fig. 4. Sketch of the artificial potential field modeling of a subject vehicle's related traffic lane marks.

in the cases of p_1 and p_2. σ_v is a coefficient of convergence on which the influence of the obstacle vehicle lies.

C. Potential of Traffic Line Marks

An automated vehicle's movement should be restricted by traffic line marks whose influence could also be described as a type of potential. There are two kinds of line marks on pavements: 1) boundary lines which do not allow vehicles to cross like l_1 and l_4 in Fig. 4, and 2) lane lines which are crossable, but may cause lateral conflicts, like l_2 and l_3. In terms of the influence of traffic line marks on a subject vehicle, the modeling of their potentials is carried out as follows.

$$l_{mn}(i) = \begin{cases} k(i) \cdot U_{lane} \cdot \exp\left(-d_{lane,i}^2 / 2\sigma_r^2\right), & i = 2, 3 \\ \sigma_r / d_{lane,i}^2, & i = 1, 4. \end{cases} \tag{4}$$

where, $k(i)$ $(i = 1, \ldots, 4)$ is a gain and U_{lane} is a coefficient of lane line's potential, σ_r is a coefficient of convergence of traffic line mark' potential and $d_{lane,i}$ represents the distance between a point and the line mark l_i $(i = 1, \ldots, 4)$ along the y-axle in the cross-section A shown in Fig. 4.

It is understandable that the potentials of lane line and boundary line are exponentially and quadratically correlated to the distance $d_{lane,i}$, respectively. These two types of potential functions reveal their influences on a subject vehicle according to traffic rules. Note that $k(i)$ is the gain for the lane line, the value of that is related to the location of the subject vehicle. For example, when the subject vehicle is traveling in the left lane, then the adjacent lane line to the subject vehicle is l_2, thus$k(2) = 1$. Since the lane line l_3 and the subject vehicle are separated by the middle lane, $k(3)$ is greater than $k(2)$, therefore take $k(3) = 2$. In another case, when the subject vehicle is driving in the middle lane, both l_2 and l_3 are the adjacent lane lines of the vehicle, then we take $k(2) = k(3) = 1$.

Therefore, the total value of the potential of traffic line marks is a combination of all the line marks' influences on the subject vehicle.

$$r_{mn} = \sum_{i=1}^{4} l_{mn}(i). \tag{5}$$

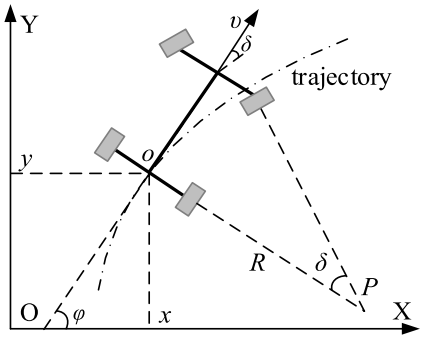

Fig. 5. Vehicle kinematic model.

D. Potential of Driving Direction

The following artificial potential field function of the subject vehicle's driving direction can induce a forward moving tendency, and force it to change lane when an obstacle appears ahead. That is to say, U-turn is not allowed in this case.

$$s_{mn} = \zeta \cdot x_r + \tau. \tag{6}$$

where, x_r is the longitudinal distance between the subject vehicle and its neighboring point in the potential field. ζ is a negative constant and τ is positive. This coefficient pair reflects that the potential's value of the vehicle's front section is lower than that in the rear, which forces the vehicle to move forward expectedly.

IV. Cooperative Control Design Based on Model Predictive Control

A. Vehicle Kinematic Modeling

A linear kinematic bicycle model considering vehicle longitudinal, lateral, and yaw motions is applied to the model predictive controller design in this study. As shown in Fig. 5, in the inertial frame XOY, x, y and φ represent three motions of the vehicle body based coordinate system with the center in the midpoint of the rear axle.

The vehicle bicycle model is obtained as follows.

$$\dot{\chi} = \begin{bmatrix} \dot{x} & \dot{y} & \dot{\varphi} \end{bmatrix}^T = \begin{bmatrix} \cos\varphi & \sin\varphi & \dfrac{1}{l}\tan\delta \end{bmatrix}^T v. \tag{7}$$

where, δ represents the front wheel steering angle, v represents the vehicle longitudinal velocity and l represents the wheel base.

We define a linear system with the system state $\chi = [x, y, \varphi]^T$, so the discretized linear system for the vehicle bicycle model is obtained as follows.

$$\chi(k+1) = \begin{bmatrix} x(k+1) \\ y(k+1) \\ \varphi(k+1) \end{bmatrix} = \begin{bmatrix} x(k) + \Delta t \cdot \upsilon(k) \cos(\varphi(k)) \\ y(k) + \Delta t \cdot \upsilon(k) \sin(\varphi(k)) \\ \varphi(k) + \Delta t \cdot \upsilon(k)/l \cdot \tan(\delta(k)) \end{bmatrix}. \tag{8}$$

where, Δt is the discrete time step, and χ $(k+1)$ represents the system state in the $(k+1)$th step. For constraints of the control increment in the model predictive controller design hereinafter, Eq. (8) should be transformed as follows.

$$\xi(k+1) = \begin{bmatrix} x(k+1) \\ y(k+1) \\ \varphi(k+1) \\ \upsilon(k+1) \\ \delta(k+1) \end{bmatrix} = \begin{bmatrix} x(k) + \Delta t \cdot \upsilon(k) \cos(\varphi(k)) \\ y(k) + \Delta t \cdot \upsilon(k) \sin(\varphi(k)) \\ \varphi(k) + \Delta t \cdot \upsilon(k)/l \cdot \tan(\delta(k)) \\ \upsilon(k) + \Delta\upsilon(k+1) \\ \delta(k) + \Delta\delta(k+1) \end{bmatrix}. \tag{9}$$

where, $\Delta u = u(k)$-$u(k$-$1)$ and it represents $[\Delta\upsilon(k),\ \Delta\delta\ (k)]^T$, while $\Delta\upsilon(k)$ and $\Delta\delta\ (k)$ represent control inputs which are the increments of vehicle velocity and front wheel steering angle in the kth step, respectively. Therefore, we use the acceleration and the front wheel steering angular velocity as the system's control inputs.

B. Model Predictive Controller Design

For the longitudinal and lateral motion control of the subject vehicle in the cooperative control system, a cost function not only reflects the vehicle's tracking performance of desired trajectories and speeds, but also consists of a weighted combination of the total value of the vehicle's potential using the aforementioned method and control increments.

$$\begin{aligned} \min J(k) = & \sum_{i=1}^{N_P} \| e_x(i) - S \|_{W_X}^2 + \sum_{i=1}^{N_P} \| e_y(i) \|_{W_Y}^2 \\ & + \sum_{i=1}^{N_P} \| e_\upsilon(i) \|_R^2 + \sum_{i=1}^{N_P} \| U_{APF}(i) \|_Q^2 \\ & + \sum_{i=0}^{N_C-1} \| \Delta u(k+i|k) \|_P^2 \\ \text{s.t. } & 0 \le \upsilon \le \upsilon_{des}, a_{\min} \le \dot{\upsilon} \le a_{\max}, \\ & -\delta_{\max} \le \delta \le \delta_{\max}, -\dot{\delta}_{\max} \le \dot{\delta} \le \dot{\delta}_{\max} \end{aligned} \tag{10}$$

where, $e_x(i)$ and $e_y(i)$ are the longitudinal and lateral errors of the predicted trajectory between the subject vehicle and its preceding vehicle in the prediction horizon N_p. $e_\upsilon(i)$ represents the error between the velocity in the prediction horizon and the desired velocity. $U_{APF}(i)$ represents the APF value in each step of the prediction horizon, the calculation method is defined by Eq.1. W_X, W_Y, R, Q, and P are weighting factors of the optimization of the MPC controller, N_p and N_c represent the prediction horizon and the control horizon. S represents the setting space between two adjacent vehicles in a platoon. $\Delta u(k+i|k)$ represents the control increment which needs to be minimized.

Note that the above cost function has two modes. When the vehicle is in single-vehicle cruising mode or as leading vehicle in multiple-vehicle platooning mode, the subject vehicle does not follow the preceding vehicle trajectory. Therefore, the $e_x(i)$ and $e_y(i)$ terms should be 0, and the desired velocity in the item $e_\upsilon(i)$ is the preset vehicle cruising speed. In this case, the cost function is also denoted as J_{cruise}. When the vehicle is a following vehicle in multiple-vehicle platooning mode, the vehicle needs to calculate the longitudinal and lateral deviation between the predicted trajectory and the preceding vehicle trajectory, i.e., $e_x(i)$ and $e_y(i)$ items, and the desired velocity in the item $e_\upsilon(i)$ is the vehicle speed in preceding vehicle trajectory. In this case, cost function is also denoted as J_{pltn}.

Moreover, for practical implementation, some constraints have been preset on the control inputs. Note that the above MPC controller may also have vehicle dynamics related constraints such as tire adhesion limit [39], [40]. However, the proposed controller is based on the vehicle kinematics model. Therefore, only the following constraints take effects in this case, i.e., the velocity υ and the front wheel steering angle δ, and their derivatives.

V. Hybrid Automata Modeling for the Cooperative Control System

As mentioned above, the cooperative control system of a vehicle platoon is a hybrid system which is a combination of several continuous vehicle motion control subsystems and a discrete maneuver switching rule for these continuous subsystems. In this case, we use hybrid automata to model the cooperative control system and set up the discrete maneuver transition rule during different traffic scenarios. Due to the complexity of hybrid traffic environments consisting of connected and non-connected (obstructive) vehicles, this transition rule and the cooperative controller should guarantee the safety of the subject vehicles even if the wireless communication for the connected vehicles is disabled. Therefore, automated vehicles have the functions of travelling alone with onboard sensors when communication is disabled and merging in a platoon when conditions met.

Aiming at the above goal, there are defined traffic events and vehicle motion states in cooperative driving scenarios. And a vehicle maneuver transition rule is presented based on hybrid automata.

A. Definitions of Traffic Events and Vehicle Motion States

In this study, we look at the automated vehicles with only two discrete maneuvers, i.e., single-vehicle cruising and multiple-vehicle platooning, so that it brings two traffic events, i.e., vehicle merging and splitting. This switch logic is simple but effective during complicated traffic scenarios when there are so many road traffic environment factors, like moving obstacles, traffic marks and related rules.

1) Definition of a Subject Vehicle's Motion States: The accomplishment of the cooperative driving depends on the perception of vehicles' motion states and their neighboring road environment information. As shown in Fig. 1, there are three

TABLE I
VEHICLE'S MOTION STATES ASSIGNMENT DURING SINGLE-VEHICLE CRUISING AND MULTIPLE-VEHICLE PLATOONING

-		*PltnEn*	*PlatoonID*	*PltnNum*	*PrecedID*	*PltnLength*
Single-vehicle cruising		1/0	Subject vehicle's *ID*	1	Subject vehicle's *ID*	1
Multiple-vehicle platooning	Leading vehicle	1	Subject vehicle's *ID*	1	Subject vehicle's *ID*	≠ PltnNum
	Following vehicles (in the middle)	1	Leading vehicle's *ID*	≠ 1	Preceding vehicle' *ID*	≠ PltnNum
	Following vehicles (in the rear)	1	Leading vehicle's *ID*	= PltnLength	Preceding vehicle' *ID*	= PltnNum

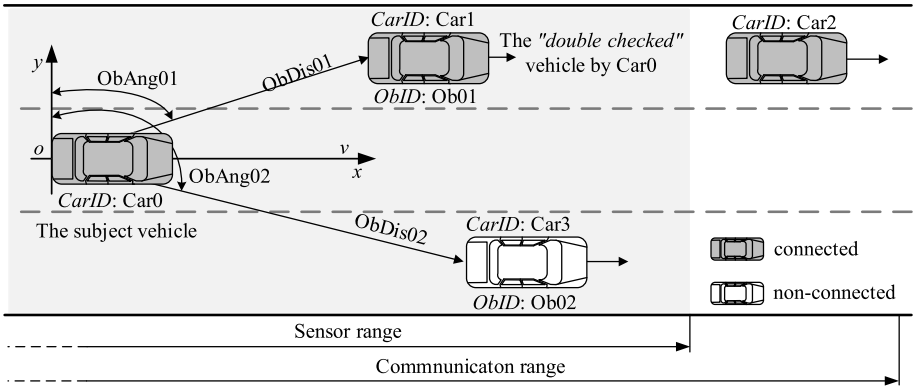

Fig. 6. The *double-check* mechanism of automated vehicles with sensors and communications.

sources of information collected for the cooperative control of single-vehicle cruising or multiple-vehicle platooning, i.e., the subject vehicle's motion states, its neighboring moving objects' motion states, as well as the traffic mark information collected with onboard sensors and wireless communications.

In order to perceive road environments effectively, we present a uniform format of two types of information through onboard sensors and wireless communications, which are assumed to be reliable and integral in this study. First, a subject vehicle's motion states collected via onboard sensors, like speed, acceleration, location, direction, traffic line marks and its obstacles' distance and azimuth angle; second, received motion states of vehicles surrounding the subject vehicle via wireless communications.

Therefore, we define a string of parameters related to vehicles' motion states for the cooperative control as:

$$CarState = [ID, Position, Dir, Speed, Acc, PltnEn, PlatoonID, PltnNum, PrecedID, PltnLength, PltnHdwy]$$

where, *ID* represents a vehicle's identifier which is exclusive in wireless communications, like a vehicle's license plate. *Position*, *Dir*, *Speed*, *Acc* represent a vehicle's position, direction, speed and longitudinal acceleration in the inertial frame XOY, respectively. *PltnEn* is a platooning enable flag which is 1 when the subject vehicle is allowed to make a platoon, and 0 when it only can cruise alone. *PlatoonID* represents the identifier of a platoon, which is equal to the subject vehicle's identifier when there is only one vehicle in the platoon

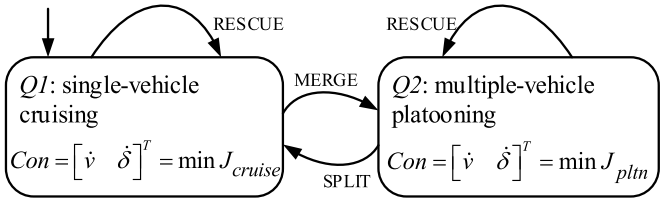

Fig. 7. Hybrid automata modeling of CDS.

(i.e. single-vehicle cruising), or equal to the leading vehicle's identifier of the platoon. *PltnNum*, *PrecedID*, *PltnLength*, and *PltnHdwy* represent the sequence number for a vehicle in a platoon, the preceding vehicle's identifier, the total number of vehicles, and the preset headway of two adjacent vehicles of a platoon, respectively. The assignments of these parameters are shown in TABLE I.

2) Definition of Data Format: In order to track the subject vehicle's neighboring vehicles and rebuild the spatial-temporal environment, we define two kinds of data string obtained through onboard sensors and wireless communications as follows.

$$Sensordata : \{Obs, ObID, ObAng, ObDis, ObPosition\}$$

where, *obs*is an identifier of data indicates that there is a neighboring obstacle vehicle's motion states sensed by onboard sensor of the subject vehicle. The following parameters, i.e., *ObID*, *ObAng*, *ObDis* and *ObPosition* represent its obstacle

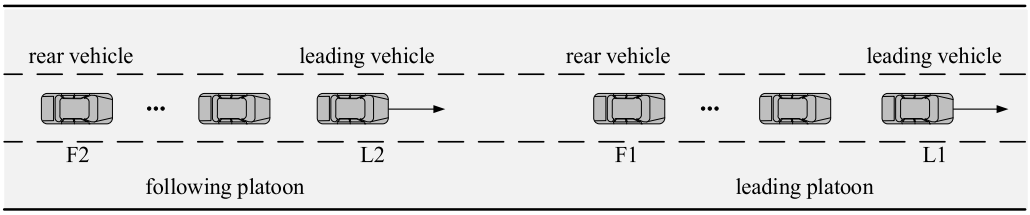

Fig. 8. Interactive relations among neighboring platoons and vehicles.

TABLE II
VARIATION OF THE SUBJECT VEHICLE'S MOTION STATES BEFORE AND AFTER THE MERGE TRANSITION

Vehicle	Transition	*PltnEn*	*PlatoonID*	*PltnNum*	*PrecedID*	*PltnLength*
L1	before	1/0	L1_ID	1	L1_ID	L1_PltnLength
	after	1/0	L1_ID	1	L1_ID	L1_PltnLength + L2_PltnLength
F1	before	1	L1_ID	F1_PltnNum	Preceding vehicle's ID	L1_PltnLength
	after	1	L1_ID	F1_PltnNum	Preceding vehicle's ID	L1_PltnLength + L2_PltnLength
L2	before	1	L2_ID	1	L2_ID	L2_PltnLength
	after	1	L1_ID	F1_PltnNum +1	F1_ID	L1_PltnLength + L2_PltnLength
F2	before	1	L2_ID	F2_PltnNum	L2_ID	L2_PltnLength
	after	1	L1_ID	F1_PltnNum + F2_PltnNum	Preceding vehicle's ID	L1_PltnLength + L2_PltnLength

TABLE III
VARIATION OF THE SUBJECT VEHICLE'S MOTION STATES BEFORE AND AFTER THE SPLIT TRANSITION

Vehicle	Transition	*PltnEn*	*PlatoonID*	*PltnNum*	*PrecedID*	*PltnLength*
L1	before	1/0	L1_ID	1	L1_ID	L1_PltnLength
	after	1/0	L1_ID	1	L1_ID	L2_PltnNum −1
F1	before	1	L1_ID	F1_PltnNum	Preceding vehicle's ID	L1_PltnLength
	after	1	L1_ID	F1_PltnNum	Preceding vehicle's ID	L2_PltnNum −1
L2	before	1	L1_ID	L2_PltnNum	F1_ID	L1_PltnLength
	after	1	L2_ID	1	L2_ID	L1_PltnLength − L2_PltnNum +1
F2	before	1	L1_ID	F2_PltnNum	L2_ID	L1_PltnLength
	after	1	L2_ID	F2_PltnNum − L2_PltnNum +1	Preceding vehicle's ID	L1_PltnLength − L2_PltnNum +1

vehicle's identifier, azimuth angle, distance relative to the subject vehicle, and location in the inertial frame.

$$Wirelessdata : \{Com, CarID, CarPosition, CarDir, CarSpeed, CarAcc, PlatoonID\}$$

where, *Com* is another identifier of data indicates that there is a neighboring vehicle whose motion states are received by wireless communication of the subject vehicle. The following parameters, i.e., *CarID*, *CarPosition*, *CarDir*, *CarSpeed*, *CarAcc* and *PlatoonID* represent its neighboring connected

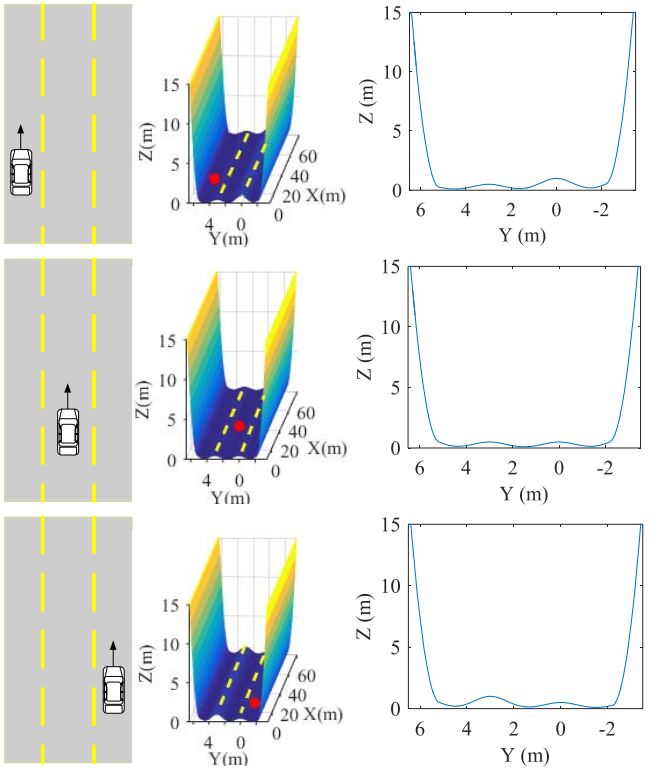

Fig. 9. Top view (left), potential view(middle) and cross-section view (right) of the subject vehicle's potential value due to traffic line marks when it drives on the left lane (top), middle lane (middle) and right lane (bottom).

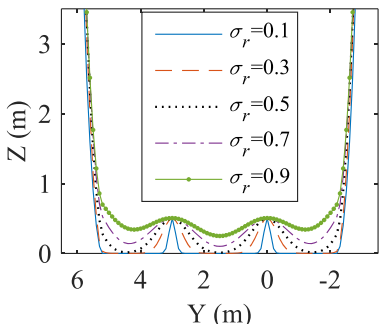

Fig. 10. Different coefficients of convergence of the traffic line mark' potentials on the subject vehicle.

vehicle's exclusive identifier, position, direction, speed, acceleration and its dependent platoon's identifier.

As shown in Fig. 6, this scenario includes four vehicles on three adjacent lanes. From the view of the subject vehicle Car0, it has both functions of a longer range of wireless communication and a shorter range of onboard sensing. There are two non-connected vehicles in its onboard sensors' range, which form two data strings with the following formats.

$$\{Obs,\ Ob01,\ ObAng01,\ ObDis01,\ ObPosition01\}$$
$$\{Obs,\ Ob02,\ ObAng02,\ ObDis02,\ ObPosition02\}.$$

In this scenario, we can see that Car1 is *double checked* by the subject vehicle Car0, excluding Car2 and Car3. Because Car1 can be "*seen*" by the subject vehicle using both its onboard sensor and wireless communication. This *double-check* mechanism is important in the process of

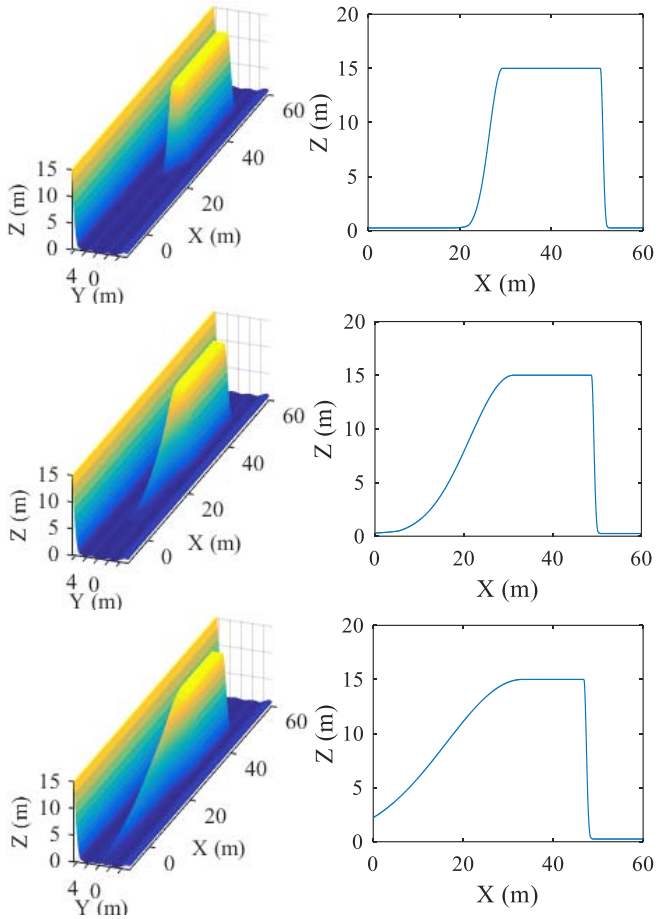

Fig. 11. Longitudinal potentials of obstacle vehicles with v_{ob} = 20m/s (top) v_{ob} = 15m/s (middle) and v_{ob} = 10m/s (bottom) exerts on the following subject vehicle with v_{host} = 22m/s.

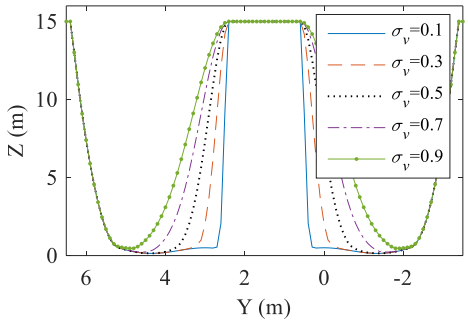

Fig. 12. Different coefficients of convergence of an obstacle vehicle's lateral potentials exerting on the subject vehicle.

multiple vehicle platooning. For traffic safety, only *double-check* vehicle can be followed by the subject vehicle to make a new platoon, which is the rule of platooning in this study.

B. Vehicle Maneuver Transition Rule

In the cooperative control system, accomplishments of single-vehicle cruising and multiple-vehicle platooning of a subject vehicle are similarly based on the model predictive control method combined with the artificial potential field approach. However, there is still a difference in terms of

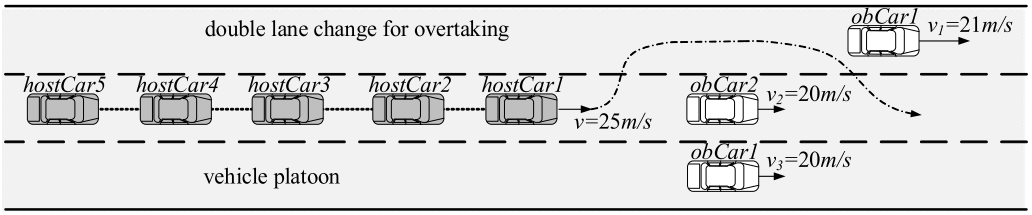

Fig. 13. Double lane change of a platoon for overtaking its front obstacle vehicles.

cost functions of two model predictive controllers. According to Eq. (10), the cost function of MPC in the single-vehicle cruising mode of the subject vehicle consists of the potential, desired speed tracking and control increment, but in the multiple-vehicle platooning mode it also includes preceding vehicle's trajectory tracking besides. Moreover, when an optimal solution cannot be obtained by the optimizer of MPC, we define a rescue event to rescue the subject vehicle with emergency braking or steering, which can improve traffic safety greatly.

A tuple H is established in terms of the syntax of hybrid automata for the cooperative control system in this study.

$$H = <Q, Var, Con, Event, Edge, Act, Inv, Init>$$

where, Q is a finite set $\{Q1, Q2\}$ of locations which represent control modes of the hybrid system (see Fig. 7). $Q1$ and $Q2$ represent single-vehicle cruising and multiple-vehicle platooning, respectively.

$Var = \{x, y, v, \varphi, \delta\}$ is a state vector of the system related to the subject vehicle and its neighboring automated vehicles.

$Con = \{\dot{v}, \dot{\delta}\}$ is the system's control vector consisting of vehicle acceleration and angular velocity of its front wheels.

$Event =$ {MERGE, SPLIT, RESCUE} is an event set of the system's transitions including vehicles merging, platoon splitting and vehicle rescuing.

Edge, *Act*, *Inv* and *Init*represent discrete maneuver transition processes, the system's continuous control subsystems and these subsystems' constraints and initial conditions, respectively.

As shown in Fig. 7, the cost functions i.e. J_{cruise} and J_{pltn}, for the MPC controllers are obtained by Eq. (10). RESCUE, MERGE and SPLIT are three events. RESCUE event is triggered when this condition is met, i.e., the maximal potential value of MPC's predicted trajectory in the prediction horizon exceeds its limit, which means there is a risk for the subject vehicle to track the predicted trajectory, for instance, some obstacles exist on the trajectory. When a RESCUE event is triggered, the subject vehicle will output the maximal deceleration control for an emergency brake to avoid collision. And we will discuss the MERGE and SPLIT events in detail hereinafter.

C. Event-Trigger Rule

For the cooperative control system using hybrid automata, a typical scenario consisting of two platoons with a leading vehicle and a rear vehicle shows the basic discrete states and events in this hybrid system (see Fig. 8). In order to elaborate the modeling process of the cooperative control system, we separately introduce the merge and split events, with considering the rescue event mentioned above.

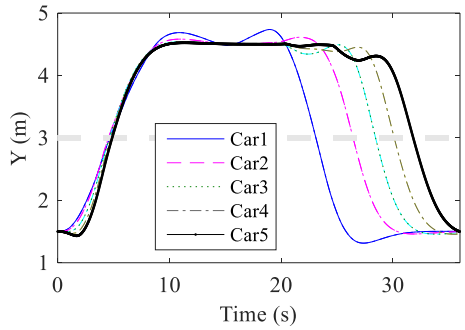

Fig. 14. Double-lane-change trajectories of the vehicles in the platoon.

1) Merge Event: For the reliability and safety of the cooperative control system, the subject vehicle has to sense and receive motion states of its front vehicle using onboard sensors and wireless communications, which is a *double-check* process, then the front vehicle becomes a candidate that can be followed to make a new platoon. From the view of the subject vehicle, the *double-check* process is accomplished through the matched speed and location of its front vehicle by both its onboard sensor and wireless communication. Further, if the candidate vehicle is cruising alone or traveling at the rear of a platoon, a merge signal will be triggered for the subject vehicle to make a new platoon, and its motion states' variations are shown in TABLE II.

In TABLE II, L1_*val* and F1_*val* represent values of serval motion states, i.e., *PlatoonID*, *PltnNum*, *PrecedID* and *PltnLength* related to the leading vehicle (L1) and the rear vehicle (F1) in the front platoon shown in Fig. 8.

2) Split Event: Unlike the simplicity of conditions to trigger the merge event, which is only accomplished by the *double-check* process using an obstacle vehicle's speed and position, there are many conditions or reasons for the subject vehicle in a platoon to split. For instance, the subject vehicle fails to *double check* its preceding vehicle, and meets its acceleration limit when its preceding vehicle is accelerating, or it is interrupted by its neighboring obstacles. Like the merge event, variations of the subject vehicle's motion states before and after the split transition are shown in TABLE III.

VI. Numerical Analysis

The cooperative control system which consists of the artificial potential field model, the model predictive controller and

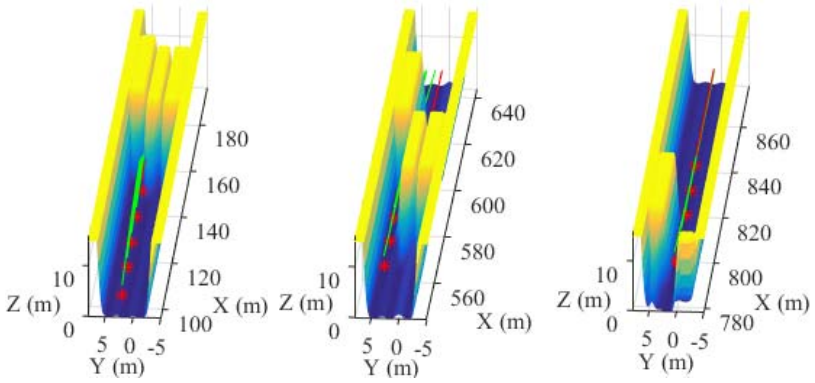

Fig. 15. Combination of traffic environments' potentials exerting on the leading vehicle at the time of 4s (left), 25s (middle), 34s (right).

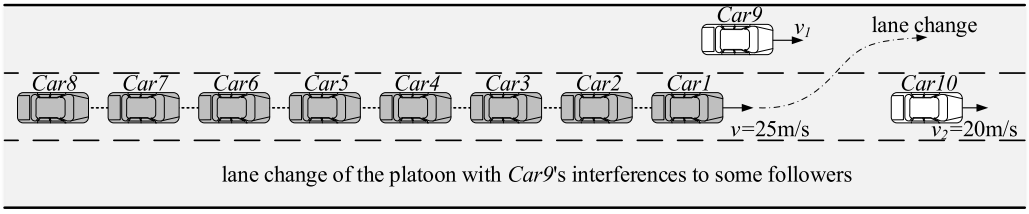

Fig. 16. Vehicle maneuver transition test scenario of the cooperative control.

the hybrid automata model based maneuver transition rule can adaptively make each vehicle switch to an optimal controlled maneuver, in terms of their surrounding road environments. Thus, the traffic capacity can be improved through vehicles' cooperative driving, with the prerequisite of driving safety.

To verify the proposed system, some numerical simulations have been conducted assuming that the onboard sensors and the wireless communications information of vehicles in a platoon can be obtained and processed appropriately.

A. Verification of Applying the Artificial Potential Field Approach

1) Vehicles' Potential Induced by Traffic Line Marks: After many times of simulation, the parameters associated with the artificial potential field algorithm are finally optimized as $U_{car} = 15$, $\sigma_v = 0.5$, $U_{lane} = 1$, $\sigma_r = 0.7$. Moreover, each member vehicle in a platoon should keep a safe clearance (headway) from its preceding vehicle. As shown in Eq. (2), we set the safe clearance $S = 0.4^* v_r + 3$, which means the time delay due to sensors and calculations is preset as 0.4s, and the minimal safe clearance is preset as 3m.

As shown in Fig. 9, the influence of the left lane line's potential on the vehicle is comparably lower than that of the right one, when it is driving on the left lane, and vice versa. Therefore, this influence of traffic line marks' potential on the subject vehicle can keep it moving on its current lane continuously.

Moreover, the coefficient of convergence σ_r has a significant impact on the shape of the subject vehicle's potential shown in Fig. 10. Taking the case that the vehicle's driving on the middle lane for example, the greater the value of σ_r is, the larger the lane lines' potential influences on the vehicle. In this study, we set $\sigma_r = 0.5$ in order to maintain a moderate influence of lane lines' potential on the vehicle.

2) Potential Induced by Surrounding Obstacle Vehicles: Taking the interaction of the platoon's leading vehicle L2 and its front obstacle vehicle F1 in Fig. 8 as an example, we can calculate the obstacle vehicle's longitudinal potential on the subject vehicle. As shown in Fig. 11, with the increasing of these two vehicles' relative speed, the influence of the obstacle vehicle's longitudinal potential on *hostCar5* extends backward and slopes much more smoothly.

Likewise, the influence of the obstacle vehicle also exerts on the subject vehicle laterally, which generates the lateral potential. We set $U_{car} = 15$, and obtain an appropriate lateral potential through adjusting the coefficient of convergence σ_v.

As shown in Fig. 12, the influence of the obstacle vehicle on the subject vehicle *hostCar5* is amplified as the value of σ_v increases. In terms of traffic rules, a moving vehicle can occupy its own traffic lane, but cannot affect adjacent lanes' vehicles which have no relative displacement to this moving vehicle laterally. Without loss of generality, we set $\sigma_v = 0.5$ which is moderate and effective in this simulation.

3) The Calculation of Potential in a Platoon: To verify the designed artificial potential field model, it is conducted a traffic scenario with a platoon composed of five connected vehicles, as well as three non-connected vehicles in front of the vehicle platoon shown in Fig. 13.

To elaborate the potential for a platoon due to its surrounding vehicles and traffic line marks, it is laid out a complex scenario shown in Fig. 13, which consists of three obstacle vehicles obCar1, obCar2 and obCar3 in front of the platoon with five connected vehicles [41]. In this scenario, we set the obstacle vehicles' speed as 21m/s, 20m/s, 20m/s, respectively, and the speeds of the vehicles in the platoon as 25m/s equally

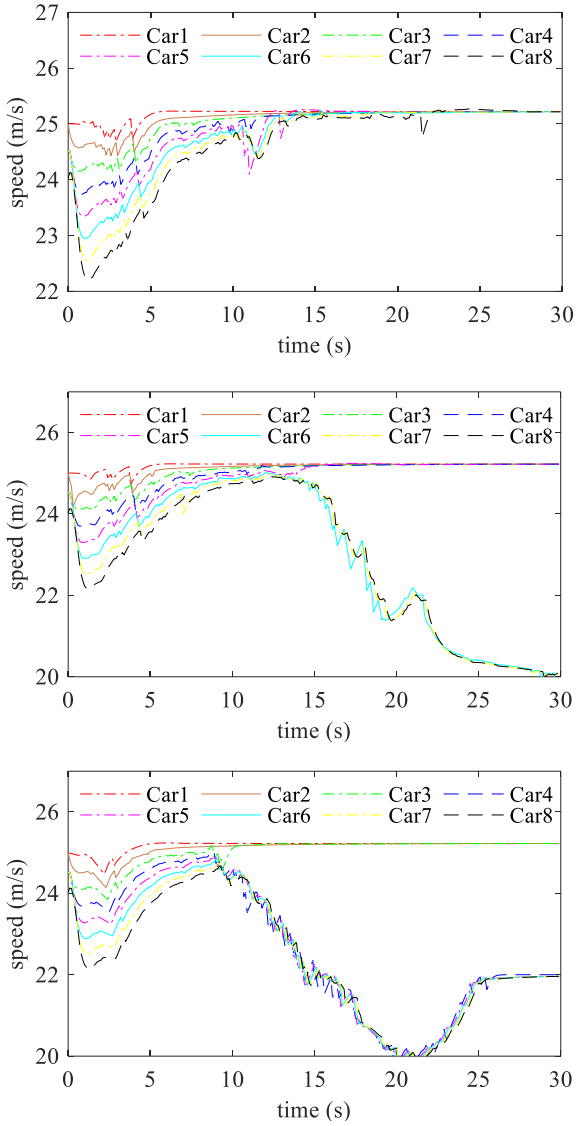

Fig. 17. Speed responses of the vehicles in the platoon when the obstacle vehicle *Car9* is at the speed of 21m/s (upper), 21.5m/s (middle) and 22m/s (bottom).

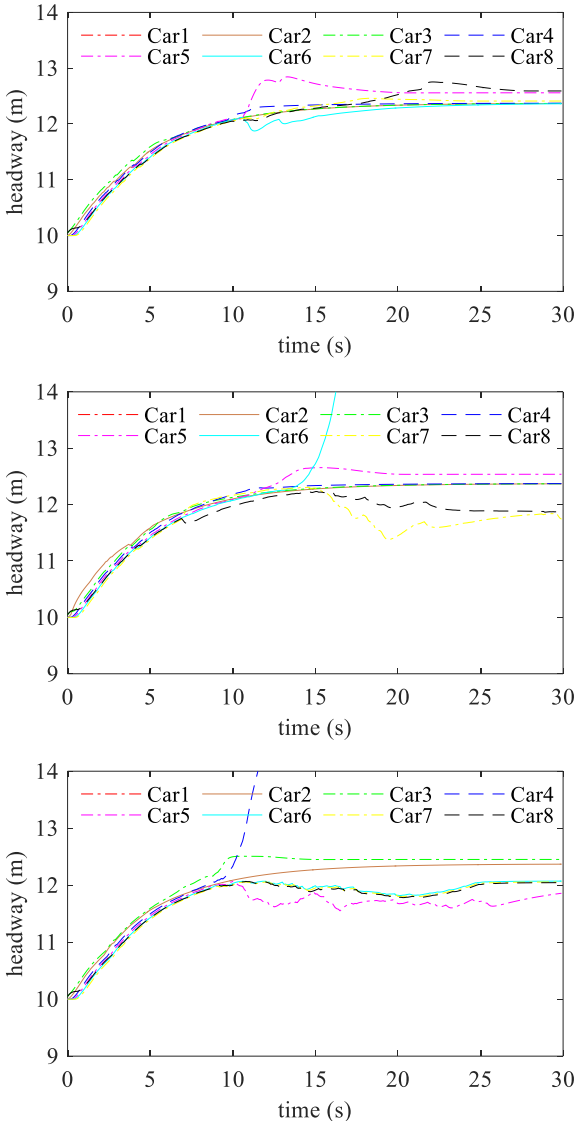

Fig. 18. Headway responses of the vehicles in the platoon when the obstacle vehicle *Car9* is at the speed of 21m/s (upper), 21.5m/s (middle) and 22m/s (bottom).

and constantly. Due to the blockages of three obstacle vehicles with lower speeds in each lane, the platoon have to make a double lane change for overtaking (see Fig. 14).

The subject vehicles named from the leading vehicle *hostCar1* to the rear vehicle *hostCar5* in the platoon with a preset speed of 25m/s to overtake the platoon's front vehicle *obCar2* with the speed of 20m/s through their first lane-change, then another lane-change for overtaking *obCar1* with the speed of 21m/s.

From the view of the leading vehicle *hostCar1* of this platoon, the potentials marked as yellow and blue areas exerted by the surrounding dynamic environments are shown in Fig. 15, in which the red line represents the leading vehicle's predicted trajectory, and the green ones represents the following vehicles' trajectories. In Fig. 15, the yellow areas spread on every lane in front of *hostCar5*, which represent the potentials generated by its three front obstacle vehicles. Similar to Fig. 11, the blue areas in this figure represent traffic line marks' potentials exerting on the leading vehicle.

In this scenario, the platoon continuously decelerates during the first 3s due to the blockage of its front moving obstacles with relatively low speeds. In the phase of 3s to 20s, with the increasing longitudinal displacement between *obCar1* and *obCar2*, the platoon automatically finds a way out because the obstacle vehicle *obCar1* on the left lane moves faster than the other two obstacle vehicles. In this case, the artificial potential field approach takes effect, it drags the platoon to the left lane where the potential value is comparably lower than the other two lanes at the same cross section of the road. In the phase of 20s to 35s, the platoon finds out that another lane change should be made to overtake, because *obCar1* in front of it still constantly moves with a relatively slow speed 21m/s. Through the double-lane-changing process, we can see that the artificial

potential field approach helps to find an optimal predicted path for the platoon.

B. Vehicle Maneuver Transition Tests of the Cooperative Control

To verify the performance of the algorithm for vehicle maneuver transitions, several scenarios with an eight-vehicle platoon and its front obstacle vehicles is carried out, which is shown in Fig. 16. In this study, all of the parameters related to the MPC controller is set as follows: the wheel-base of the simulated vehicle $l = 2.7$m, the negative coefficient of the potential $\zeta = -0.01$.

positive coefficient of the potential $\tau = 2$, sample time $T = 0.02$s, predict control time $T_p = 0.25$s, control horizon $N_c = 2$, predict horizon $N_p = 25$, weight of the potential $Q = 5$, weight of the speed error $R = 1$, weight of the control increment $P = 6$, weight of the lateral tracking error $W_Y = 1.5$, weight of the longitudinal tracking error $W_X = 2$, lower limit of the acceleration $a_{\min} = -4.9$ m/s^2, upper limit of the acceleration $a_{\max} = 1$ m/s^2, maximum steering angle $\delta_{\max} = 25°$, maximum steering angular speed $\dot{\delta}_{max} = 9.4°$/s.

The platoon's speed is set as 25 m/s, and 20m/s for the obstacle vehicle*Car10* right ahead of the platoon. Through adjusting *Car9*'s speed as 21m/s, 21.5m/s and 22m/s, some following vehicles in the platoon may have to stop changing lane to avoid possible collisions with *Car9* due to its interference at the target lane [41]. In these three scenarios, the vehicles in the platoon may have to make maneuver transitions from the multiple-vehicle platooning to the single-vehicle cruising (a leading vehicle of a new platoon), i.e. the platoon is split as two new platoons, in which the front platoon successfully finishes a lane change but the following one fails.

Through the simulation test of these three scenarios, we can see that different speed of the obstacle vehicle *Car9* leads to a different maneuver of each vehicle in the platoon. With the increasing of *Car9*'s speed, its interference can cause different position of separation. The greater the obstacle vehicle *Car9*'s speed is, the closer the separation location is relative to the leading vehicle. If *Car9*'s speed is large enough, all of the member vehicles in the platoon will fail to change lane until the interference disappears. It turns out that the whole platoon successfully makes the lane change maneuver when *Car9*'s speed is 21m/s, but some member vehicles fail when *Car9*'s speed is 21.5m/s and 22m/s, which form a new platoon with the leading vehicle *Car6* and *Car4*, respectively. The responses of vehicle motion states, like the speed responses, the headway responses, the lateral deviation responses and the platoon ID responses, during the lane change of the platoon with the interference of the obstacle vehicles *Car9* and *Car10* are shown in Fig. 17, Fig. 18, Fig. 19 and Fig. 20, respectively.

These responses show that all the member vehicles can maintain stable motion states with minor trembles during the lane change maneuver in the first scenario with *Car9*'s speed of 21m/s. However, in the other two scenarios, some member vehicles have to make a maneuver transition from the multiple-vehicle platooning mode to the single-vehicle cruising mode, forming new platoons.

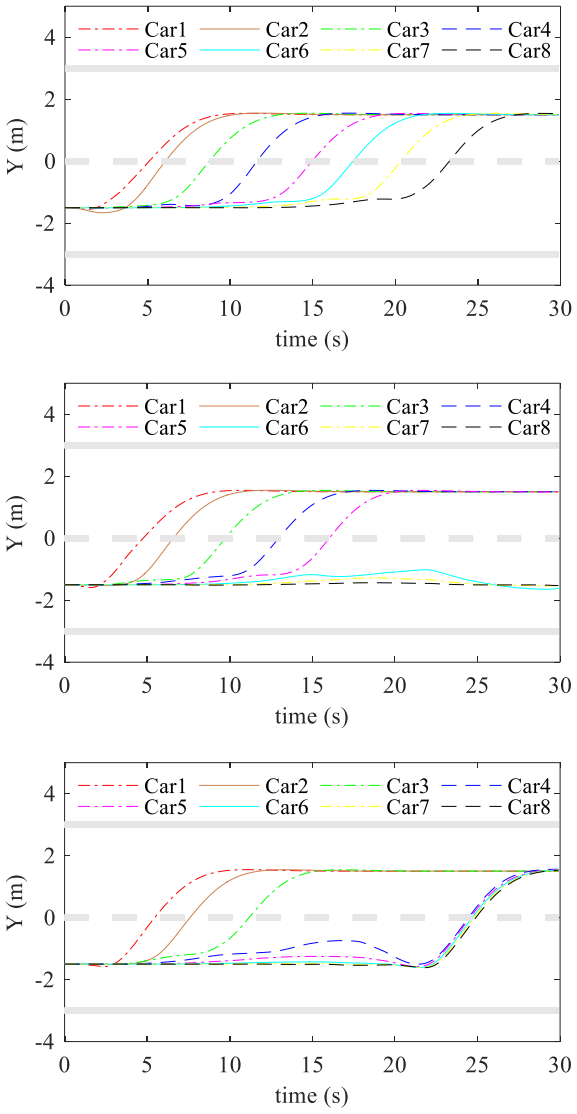

Fig. 19. Lateral deviation responses of the vehicles in the platoon when the obstacle vehicle *Car9* is at the speed of 21m/s (upper), 21.5m/s (middle) and 22m/s (bottom).

As shown in Fig. 18, the front headways of *Car6* and *Car4* begin to diverge at the 15th and 10th second, respectively; Fig.20 shows that they become the leading vehicles of new platoons in these two scenarios at the 21.7th and 17.3th second. From the speed responses in Fig. 17 and the lateral deviation responses in Fig. 19, we can see that only five member vehicles *Car1*∼*Car5* successfully make the lane changes and maintain the speed 25m/s, but other member vehicles *Car6*∼*Car8* fail and decrease to their obstacle vehicle's speed 20m/s, during the rest of the simulation phase.

In the third scenario when *Car9*'s speed increases to 22m/s, we can see from Fig. 19 that three member vehicles *Car1*∼*Car3* firstly make the lane change maintaining the speed of 22m/s. Moreover, the other member vehicles *Car4*∼*Car8* in the original platoon form a new platoon, due to the interference of *Car9* to the leading vehicle *Car4*. As shown in Fig. 17, the new platoon firstly decreases to its obstacle

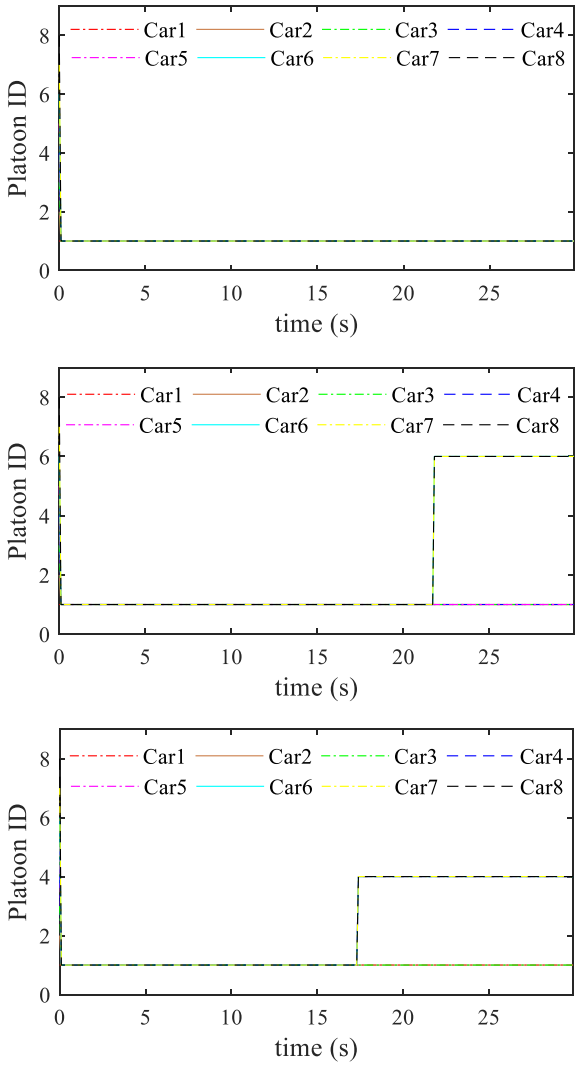

Fig. 20. Platoon ID responses of the vehicles in the platoon when the obstacle vehicle Car9 is at the speed of 21m/s (upper), 21.5m/s (middle) and 22m/s (bottom).

vehicle *Car10*'s speed of 20m/s, then increases to the obstacle vehicle *Car9*'s speed of 22m/s after the complete of its lane change maneuver.

C. Discussion

Automated driving control can generally be divided into three parts, namely perception, planning and tracking. In the real road environment, one of the major difficulties in automated driving control is how to deal with various randomness in every link of control. These randomness include the randomness of sensor errors, the communication delay, and other vehicles or pedestrians in the traffic environment. This paper mainly aims at the interactions of automated vehicles, including the connected and the non-connected vehicles. By establishing the function of artificial potential field combined with the model predictive control, the traffic behavior of other vehicles on the road can be predicted in advance to solve the randomness of other vehicles in traffic environment. From the simulation in chapter VI, we can see that the proposed cooperative control algorithm can not only realize single-vehicle cruise control, but also flexibly realize the merge and split maneuvers of a platoon in terms of the random conditions.

In this paper, it assumes that the vehicle has good sensor and communication, and we do not look into the influence of the randomness of sensor and communication errors on the system. However, one of the major characteristics of the proposed model predictive control algorithm is that it can deal with the model mismatch problem to some extent. In fact, for the simulation in Chapter VII, there is 10% random error added to the control input. The result shows the robustness of the proposed algorithm.

VII. Conclusion

The vehicle cooperative driving system is a typical hybrid system, consisting of transitions of discrete vehicle maneuvers and the continuous vehicle motion control. In this paper, it's proposed a dual-layered hybrid control structure whose upper layer is in charge of the transition of discrete vehicle maneuvers, and the lower layer is responsible for the continuous vehicle motion control. Moreover, the cooperative driving system is distributed since each automated vehicle in a platoon is independently controlled by itself, only sharing real-time motion states and other cooperative information, like when and where for a vehicle to change its maneuver.

The artificial potential field approach is applied for path planning of single automated vehicle in traffic environments. In detail, the potential for an automated vehicle is a combination of force-like influences exerted on it by its surrounding traffic elements including obstacle vehicles, traffic line marks, as well as driving directions. A model predictive controller is designed, combined with a vehicle' potential, to solve the control problem with multiple inputs and constrains. Therefore, this MPC controller can help to look for an optimal path using its optimizer, and track this path by adjusting its control outputs concurrently. Another advantage of this controller is that the gradient-descending method used in traditional artificial potential field approach is replaced by the optimizer of MPC to tackle the problem of local minima.

For decision-making of transiting discrete vehicle maneuvers, we elaborate a switching strategy between automated vehicles' merge and split, based on hybrid automata. That is to say, we let automated vehicles in a platoon only have two switchable maneuvers, i.e. single-vehicle cruising and multiple-vehicle platooning, whose transitions can lead to vehicles' merge or split events, respectively. This feature simplifies the transition rule and improves the transition efficiency of automated vehicles during complex traffic scenarios. Through some comparative simulation tests, we can see that the designed MPC controller and the presented transition rule can effectively handle typical traffic situations in which there are connected or non-connected vehicles (obstacles) interfering an automated platoon's normal travels. In addition, different speeds of obstacles lead to different maneuver transitions of member vehicles in the platoon to avoid possible collisions.

In summary, CDS with automated vehicle platoons can not only increase the traffic capacity due to vehicles' interactions,

but also improve the traffic safety by using each automated vehicle's capability of collision avoidance. In future, we will continue to optimize the algorithm functional of path planning and cooperative control by replacing with more precise vehicle dynamics model which may lead to the implementation of an improved MPC controller.

REFERENCES

[1] L. Blincoe, T. Miller, E. Zaloshnja, and B. A. Lawrence, "The economic and societal impact of motor vehicle crashes, 2010, (revised)," Nat. Highway Traffic Saf. Admin., Washington, DC, USA, Tech. Rep. DOT HS 812 013, 2015.

[2] A. C. Mersky and C. Samaras, "Fuel economy testing of autonomous vehicles," *Transp. Res. C, Emerg. Technol.*, vol. 65, pp. 31–48, Apr. 2016.

[3] K.-Y. Liang, J. Mårtensson, and K. H. Johansson, "Heavy-duty vehicle platoon formation for fuel efficiency," *IEEE Trans. Intell. Transp. Syst.*, vol. 17, no. 4, pp. 1051–1061, Apr. 2016.

[4] D. Moser, R. Schmied, H. Waschl, and L. del Re, "Flexible spacing adaptive cruise control using stochastic model predictive control," *IEEE Trans. Control Syst. Technol.*, vol. 26, no. 1, pp. 114–127, Jan. 2018.

[5] T. Haran and S. Chien, "Infrared reflectivity of pedestrian mannequin for autonomous emergency braking testing," in *Proc. IEEE 19th Int. Conf. Intell. Transp. Syst. (ITSC)*, Nov. 2016, pp. 2230–2235.

[6] J. Kim, W. Y. Jung, S. Kwon, and Y. Kim, "Performance test of autonomous emergency braking system based on commercial radar," in *Proc. 5th IIAI Int. Congr. Adv. Appl. Inform. (IIAI-AAI)*, 2016, pp. 1211–1212.

[7] G. Savino, J. Brown, M. Rizzi, M. Pierini, and M. Fitzharris, "Triggering algorithm based on inevitable collision states for autonomous emergency braking (AEB) in motorcycle-to-car crashes," in *Proc. IEEE Intell. Vehicles Symp. (IV)*, Jun./Jul. 2015, pp. 1195–1200.

[8] C. Liu, A. Carvalho, G. Schildbach, and J. K. Hedrick, "Stochastic predictive control for lane keeping assistance systems using a linear time-varying model," in *Proc. Amer. Control Conf. (ACC)*, 2015, pp. 3355–3360.

[9] N. M. Enache, Y. Sebsadji, S. Mammar, B. Lusetti, and S. Glaser, "Driver's influence on the performance of an integrated lane departure avoidance and lane keeping assistance system," in *Proc. IEEE Control Appl. (CCA), Intell. Control (ISIC)*, Jul. 2009, pp. 119–124.

[10] N. Kalra and S. M. Paddock, "Driving to safety: How many miles of driving would it take to demonstrate autonomous vehicle reliability?" *Transp. Res. A, Policy Pract.*, vol. 94, pp. 182–193, Dec. 2016.

[11] S.-W. Kim *et al.*, "Multivehicle cooperative driving using cooperative perception: Design and experimental validation," *IEEE Trans. Intell. Transp. Syst.*, vol. 16, no. 2, pp. 663–680, Apr. 2015.

[12] S. Fujii *et al.*, "Cooperative vehicle positioning via V2V communications and onboard sensors," in *Proc. IEEE Veh. Technol. Conf. (VTC)*, Sep. 2011, pp. 1–5.

[13] A. I. M. Medina, N. van de Wouw, and H. Nijmeijer, "Automation of a T-intersection using virtual platoons of cooperative autonomous vehicles," in *Proc. IEEE 18th Int. Conf. Intell. Syst.*, Sep. 2015, pp. 1696–1701.

[14] S. Öncü, J. Ploeg, N. van de Wouw, and H. Nijmeijer, "Cooperative adaptive cruise control: Network-aware analysis of string stability," *IEEE Trans. Intell. Transp. Syst.*, vol. 15, no. 4, pp. 1527–1537, Aug. 2014.

[15] Y. A. Harfouch, S. Yuan, and S. Baldi, "An adaptive switched control approach to heterogeneous platooning with inter-vehicle communication losses," *IEEE Trans. Control Netw. Syst.*, to be published.

[16] D. Caveney, "Cooperative vehicular safety applications," *IEEE Control Syst.*, vol. 30, no. 4, pp. 38–53, Aug. 2010.

[17] P. Koopman and M. Wagner, "Autonomous vehicle safety: An interdisciplinary challenge," *IEEE Intell. Transp. Syst. Mag.*, vol. 9, no. 1, pp. 90–96, Jan. 2017.

[18] S. Hallé and B. Chaib-draa, "A collaborative driving system based on multiagent modelling and simulations," *Transp. Res. C, Emerg. Technol.*, vol. 13, no. 4, pp. 320–345, 2005.

[19] C. G. Cassandras, "From discrete event to hybrid systems," in *Proc. 6th Int. Workshop Discrete Event Syst.*, 2002, pp. 3–8.

[20] H. Raza and P. Ioannou, "Vehicle following control design for automated highway systems," *IEEE Control Syst.*, vol. 16, no. 6, pp. 43–60, Dec. 1996.

[21] P. Kachroo and Z. Li, "Vehicle merging control design for an automated highway system," in *Proc. Conf. Intell. Transp. Syst.*, 1997, pp. 224–229.

[22] R. Horowitz and P. Varaiya, "Control design of an automated highway system," *Proc. IEEE*, vol. 88, no. 7, pp. 913–925, Jul. 2000.

[23] S. Tsugawa, S. Kato, T. Matsui, H. Naganawa, and H. Fujii, "An architecture for cooperative driving of automated vehicles," in *Proc. ITSC IEEE Intell. Transp. Syst.*, Oct. 2000, pp. 422–427.

[24] L. Iftekhar and R. Olfati-Saber, "Autonomous driving for vehicular networks with nonlinear dynamics," in *Proc. IEEE Intell. Vehicles Symp.*, Jun. 2012, pp. 723–729.

[25] O. Khatib, "Real-time obstacle avoidance for manipulators and mobile robots," in *Proc. IEEE Int. Conf. Robot. Autom. Proc.*, vol. 2, Mar. 1985, pp. 500–505.

[26] R. Raja, A. Dutta, and K. S. Venkatesh, "New potential field method for rough terrain path planning using genetic algorithm for a 6-wheel rover," *Robot. Auton. Syst.*, vol. 72, pp. 295–306, Oct. 2015.

[27] E. Semsar-Kazerooni, J. Verhaegh, J. Ploeg, and M. Alirezaei, "Cooperative adaptive cruise control: An artificial potential field approach," in *Proc. IEEE Intell. Vehicles Symp. (IV)*, Jun. 2016, pp. 361–367.

[28] Y. Rasekhipour, A. Khajepour, S.-K. Chen, and B. Litkouhi, "A potential field-based model predictive path-planning controller for autonomous road vehicles," *IEEE Trans. Intell. Transp. Syst.*, vol. 18, no. 5, pp. 1255–1267, May 2017.

[29] M. T. Wolf and J. W. Burdick, "Artificial potential functions for highway driving with collision avoidance," in *Proc. IEEE Int. Conf. Robot. Autom.*, May 2008, pp. 3731–3736.

[30] X. Li, Z. Sun, D. Cao, D. Liu, and H. He, "Development of a new integrated local trajectory planning and tracking control framework for autonomous ground vehicles," *Mech. Syst. Signal Process.*, vol. 87, pp. 118–137, Mar. 2017.

[31] X.-G. Guo, J.-L. Wang, F. Liao, and R. S. H. Teo, "String stability of heterogeneous leader-following vehicle platoons based on constant spacing policy," in *Proc. IEEE Intell. Vehicles Symp. (IV)*, Jun. 2016, pp. 761–766.

[32] V. Milanés, S. E. Shladover, J. Spring, C. Nowakowski, H. Kawazoe, and M. Nakamura, "Cooperative adaptive cruise control in real traffic situations," *IEEE Trans. Intell. Transp. Syst.*, vol. 15, no. 1, pp. 296–305, Feb. 2014.

[33] D. Yang, L. Zhu, B. Ran, Y. Pu, and P. Hui, "Modeling and analysis of the lane-changing execution in longitudinal direction," *IEEE Trans. Intell. Transp. Syst.*, vol. 17, no. 10, pp. 2984–2992, Oct. 2016.

[34] D. Bevly *et al.*, "Lane change and merge maneuvers for connected and automated vehicles: A survey," *IEEE Trans. Intell. Veh.*, vol. 1, no. 1, pp. 105–120, Mar. 2016.

[35] M. Düring, K. Franke, R. Balaghiasefi, M. Gonter, M. Belkner, and K. Lemmer, "Adaptive cooperative maneuver planning algorithm for conflict resolution in diverse traffic situations," in *Proc. Int. Conf. Connected Vehicles Expo (ICCVE)*, 2014, pp. 242–249.

[36] M. Suzuki, R. Harada, S. Kanda, and H. Shigeno, "Overtaking priority management method between platoons and surrounding vehicles considering carbon dioxide emissions (poster)," in *Proc. IEEE Veh. Netw. Conf. (VNC)*, Nov. 2011, pp. 260–267.

[37] Z. Wang, G. Wu, and M. J. Barth, "Developing a distributed consensus-based cooperative adaptive cruise control system for heterogeneous vehicles with predecessor following topology," *J. Adv. Transp.*, vol. 2017, Jun. 2017, Art. no. 1023654.

[38] S. E. Li *et al.*, "Performance enhanced predictive control for adaptive cruise control system considering road elevation information," *IEEE Trans. Intell. Vehicles*, vol. 2, no. 3, pp. 150–160, Sep. 2017.

[39] A. Bayuwindra, Ø. L. Aakre, J. Ploeg, and H. Nijmeijer, "Combined lateral and longitudinal CACC for a unicycle-type platoon," in *Proc. IEEE Intell. Vehicles Symp.(IV)*, Jun. 2016, pp. 527–532.

[40] A. F. Idriz, A. S. A. Rachman, and S. Baldi, "Integration of auto-steering with adaptive cruise control for improved cornering behaviour," *IET Intell. Transp. Syst.*, vol. 11, no. 10, pp. 667–675, 2017.

[41] D. Chu. (2017). *The Cooperative Driving System (Video)*. [Online]. Available: https://youtu.be/4QnXU0HBLOM

Zichao Huang received the B.E., M.S., and Ph.D. degrees from Wuhan University of Technology, Wuhan, China, in 2010, 2013 and 2016, respectively, all in mechanical engineering.

He is currently a Post-Doctoral Fellow with the Research Institute of Highway, Ministry of Transport of China. His research interests include autonomous vehicle, cooperative driving, and automated vehicle test methods.

Duanfeng Chu received the B.E. and Ph.D. degrees in mechanical engineering from Wuhan University of Technology, Wuhan, China, in 2005 and 2010, respectively.

He has visited California PATH, University of California at Berkeley, Berkeley, USA, and The Ohio State University, USA, in 2009 and 2017, respectively. He is currently an Associate Professor with the Intelligent Transportation Systems Research Center, Wuhan University of Technology, focusing on the research of automated and connected vehicle and intelligent transportation systems.

Dr. Chu has been a reviewer for several international journals and conferences in the field of automated vehicle.

Chaozhong Wu received the B.E. degree in marine engineering, the M.S. degree in management science and engineering, and the Ph.D. degree in transportation engineering from Wuhan University of Technology, Wuhan, China, in 1996, 1999 and 2002, respectively.

He was a Visiting Scholar with University of Regina, Canada, and Northeastern University, USA, in 2006 and 2015, respectively. He is currently a Professor and the Director with the Intelligent Transportation Systems Research Center, Wuhan University of Technology. He is an expert in traffic safety, connected vehicle, and intelligent transportation systems. He has authored over 60 journal articles and holds 11 patents.

Dr. Wu was a recipient of the New Century Excellent Talent of Ministry of Education of China in 2010, the Young Talent of Ministry of Transport of China in 2012, the Distinguished Young Scholar of Hubei Province of China in 2012, and the Young Leading Talent of Ministry of Transport of China in 2014. He serves as an associate editor for some journals.

Yi He received the Ph.D. degree in intelligent transportation system engineering from Wuhan University of Technology, China in 2015. Since 2017, he has been with California PATH, University of California at Berkeley, Berkeley, CA, USA. He is currently an Assistant Professor with the Intelligent Transportation System Research Center, Wuhan University of Technology. His research interests include vehicle safety and driving behavior.